Supporting information

Curcumin based ionic Pt(II) complexes:

antioxidant and antimicrobial activity

Rossella Caligiuri,[a] Giuseppe Di Maio,[a,b] Nicolas Godbert,[a] Francesca Scarpelli,[a] Angela Candreva,[a] Isabella Rimoldi,[c] Giorgio Facchetti,[c] Maria Giovanna Lupo,[d] Emilia Sicilia,[e] Gloria Mazzone,[e] Fortuna Ponte,[e] Isabella Romeo,[f,g] Massimo La Deda,[a,b] Alessandra Crispini,[a] Renata De Rose[h] and Iolinda Aiello*[a,b]

[a] MAT-INLAB, LASCAMM CR-INSTM, Unità INSTM della Calabria, Dipartimento di Chimica e Tecnologie Chimiche, Università della Calabria, Ponte Pietro Bucci Cubo 14C, Arcavacata di Rende (CS), 87036, Italy, E-mail: iolinda.aiello@unical.it

[b] CNR NANOTEC-Istituto di Nanotecnologia UOS Cosenza, Arcavacata di Rende (CS), 87036, Italy

[c] Dipartimento di Scienze Farmaceutiche, Università degli Studi di Milano, Via Venezian 21, Milan, 20133, Italy

[d] *Dipartimento di Medicina, Università degli Studi di Padova, 35128 Padova, Italy*

[e] *Dipartimento di Chimica e Tecnologie Chimiche, Ponte Pietro Bucci Cubo 14C, Arcavacata di Rende (CS), 87036, Italy*

[f] Dipartimento di Scienze della Salute, Università degli Studi "Magna Græcia" di Catanzaro, Campus "S. Venuta", Viale Europa, 88100 Catanzaro, Italy

[g] Net4Science Academic Spin-Off, Università degli Studi "Magna Græcia" di Catanzaro, Campus "S. Venuta", Viale Europa, 88100 Catanzaro, Italy

[h] LAB CF-INABEC Dipartimento di Chimica e Tecnologie Chimiche, Ponte Pietro Bucci Cubo 15C, Arcavacata di Rende (CS), 87036, Italy

Table of Contents

Figure S35: Thermodynamic parameters: bond dissociation enthalpies (BDE, grey), electron transfer enthalpies (ETE, light violet), adiabatic ionization potentials (IP, red), O-H proton dissociation enthalpies (PDE, blue) and proton affinities (PA, green), at 298.15 K.

Table S2: ADME properties for H(curc) and Pt(II) complexes **1**-**4**.

Table S3. Theoretical and experimental $logP_{ow}$ values of the Pt(II) complexes **1**-**4**.

Figure S36: BOILED-Egg Model of complexes **1**-**3**.

Table S4: Antimicrobial activity data against *E. coli* and *S. aureus*.

Figure S37: Inhibition halos on *S. aureus* (A) and *E. Coli* (B) at 0.5 µg/µl. C: H(curc).

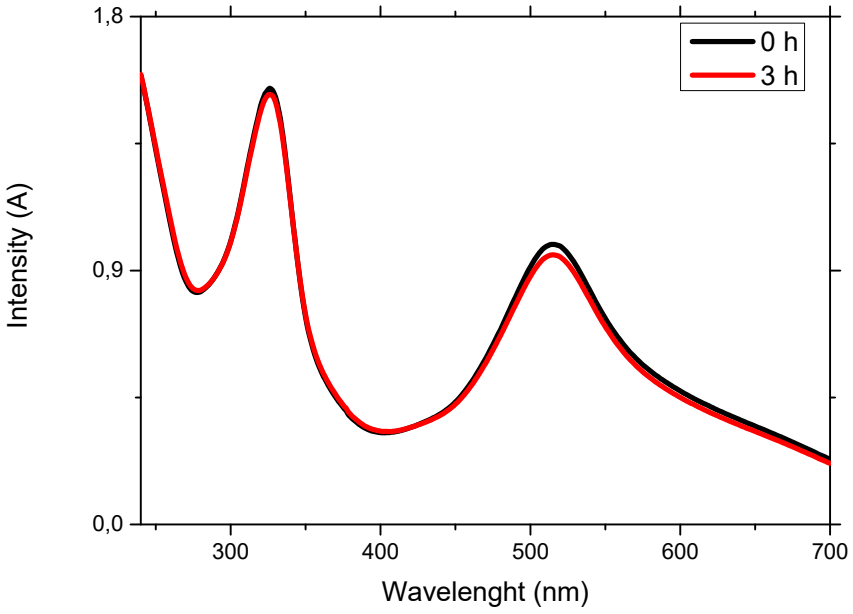

Figure S1: Absorption spectra of **DPPH** in MeOH dilute solution (100 µM) varying time.

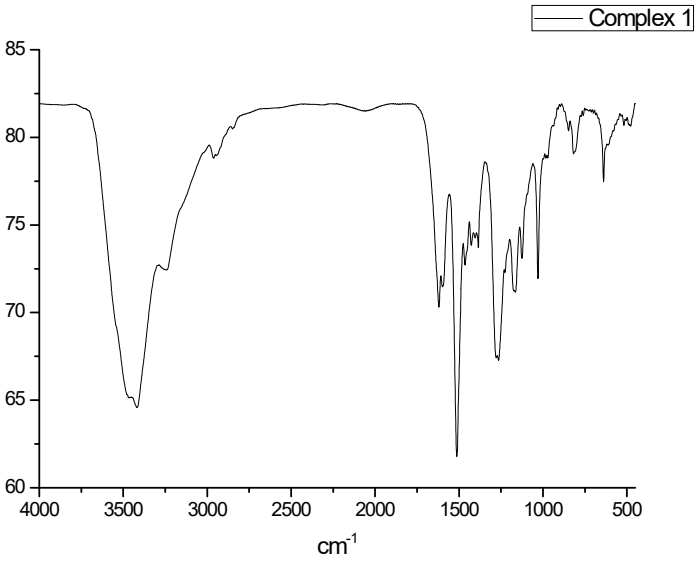

Figure S2: FT-IR spectrum of complex [(pn)Pt(curc)][CF_3SO_3], **1**.

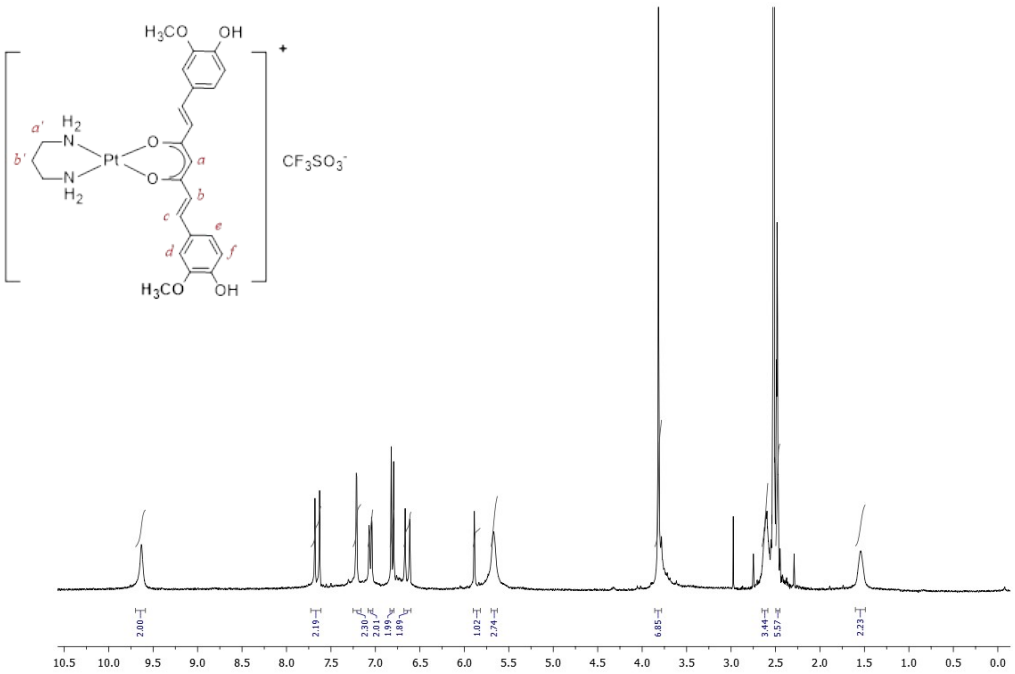

Figure S3: ^{1}H-NMR spectrum of complex [(pn)Pt(curc)][CF_3SO_3], **1**.

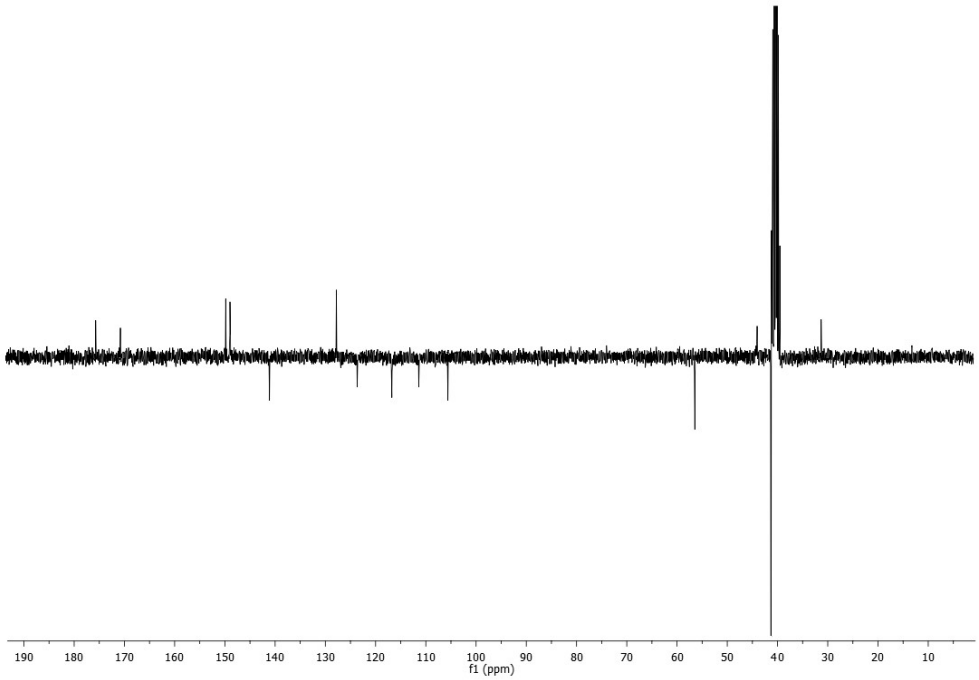

Figure S4: ^{13}C-NMR spectrum of complex [(pn)Pt(curc)][CF_3SO_3], **1**.

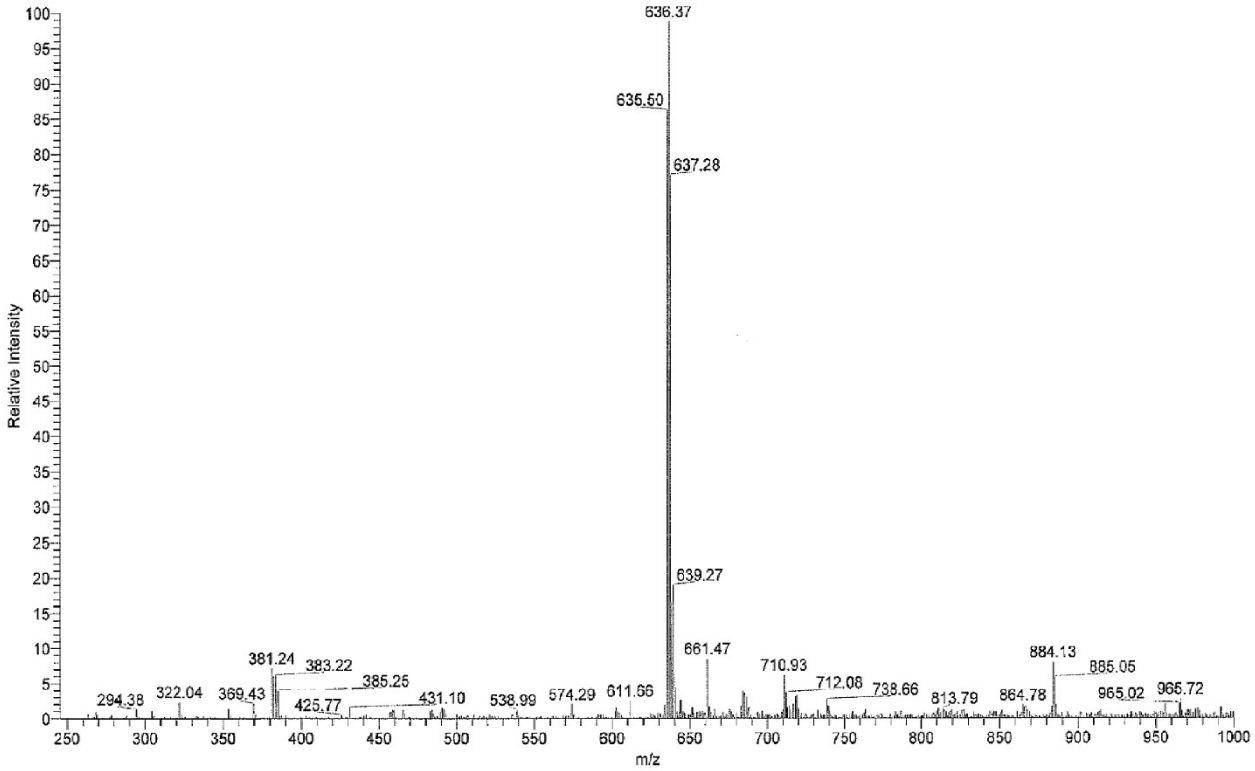

Figure S5: MS spectrum of complex [(pn)Pt(curc)][CF_3SO_3], **1**

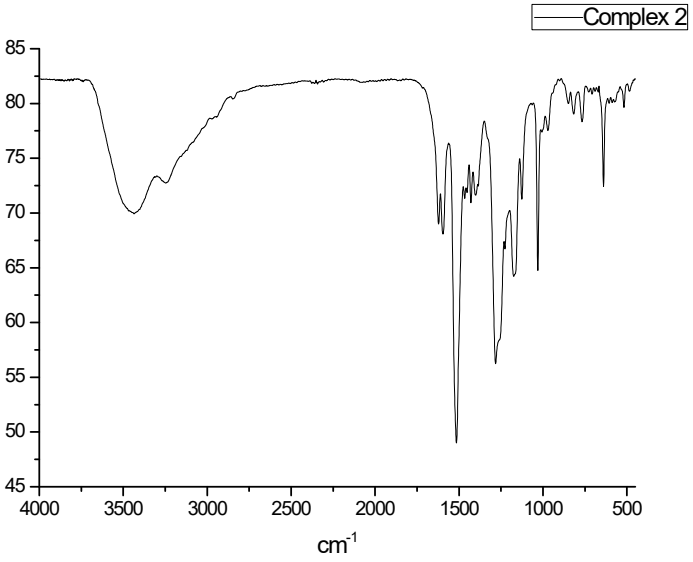

Figure S6: FT-IR spectrum of complex [(pic)Pt(curc)][CF_3SO_3], **2**.

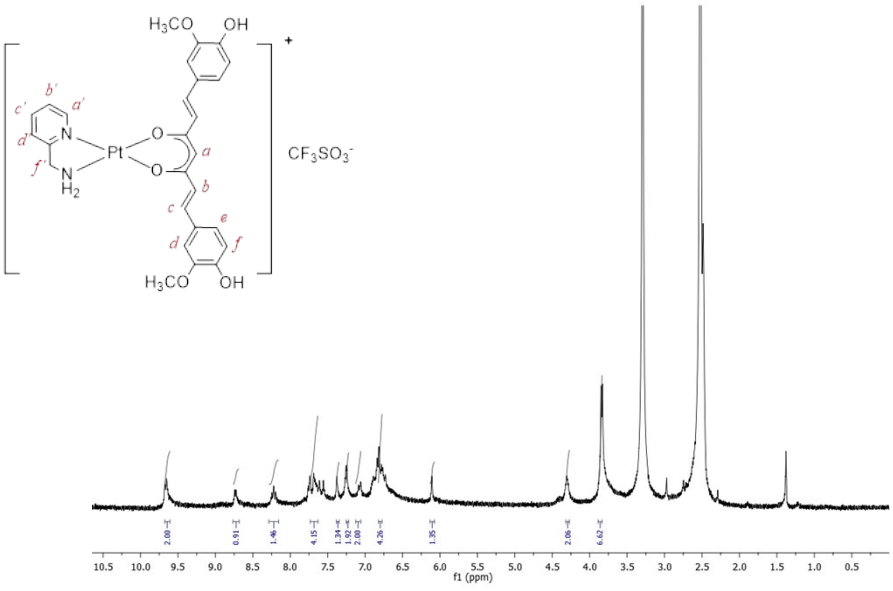

Figure S7: ^{1}H-NMR spectrum of complex [(pic)Pt(curc)][CF_3SO_3], **2**.

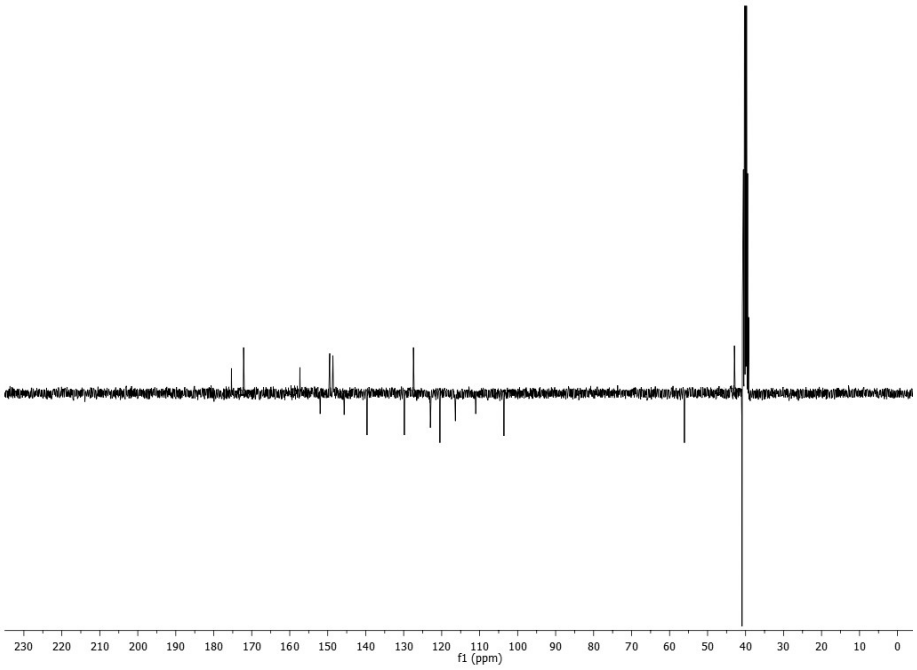

Figure S8: ^{13}C-NMR spectrum of complex [(pic)Pt(curc)][CF_3SO_3], **2**.

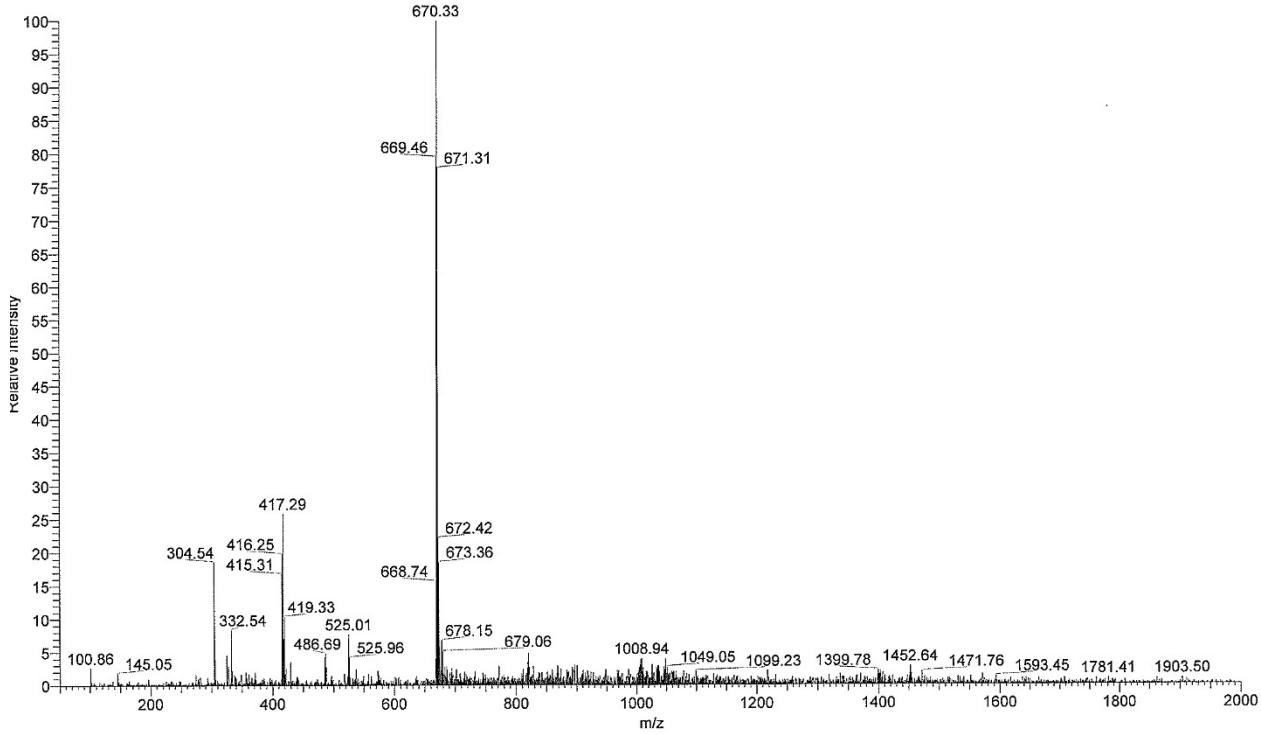

Figure S9: MS spectrum of complex [(pic)Pt(curc)][CF_3SO_3], **2**.

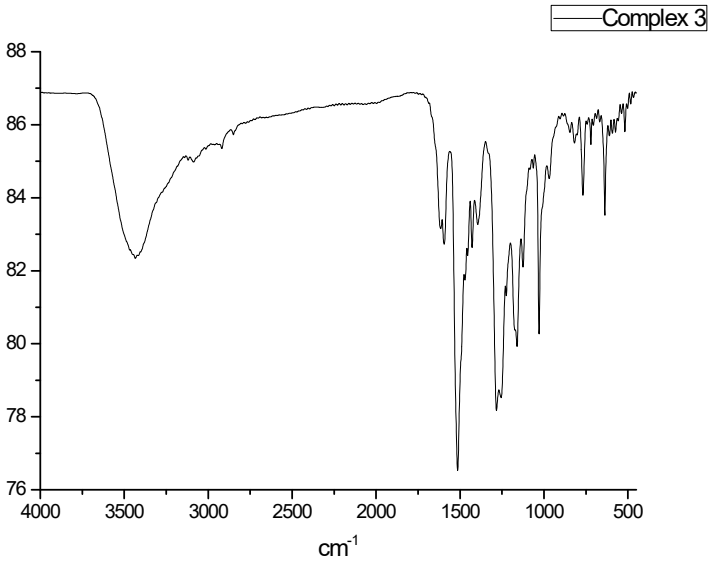

Figure S10: FT-IR spectrum of complex[(bipy)Pt(curc)][CF_3SO_3], **3**.

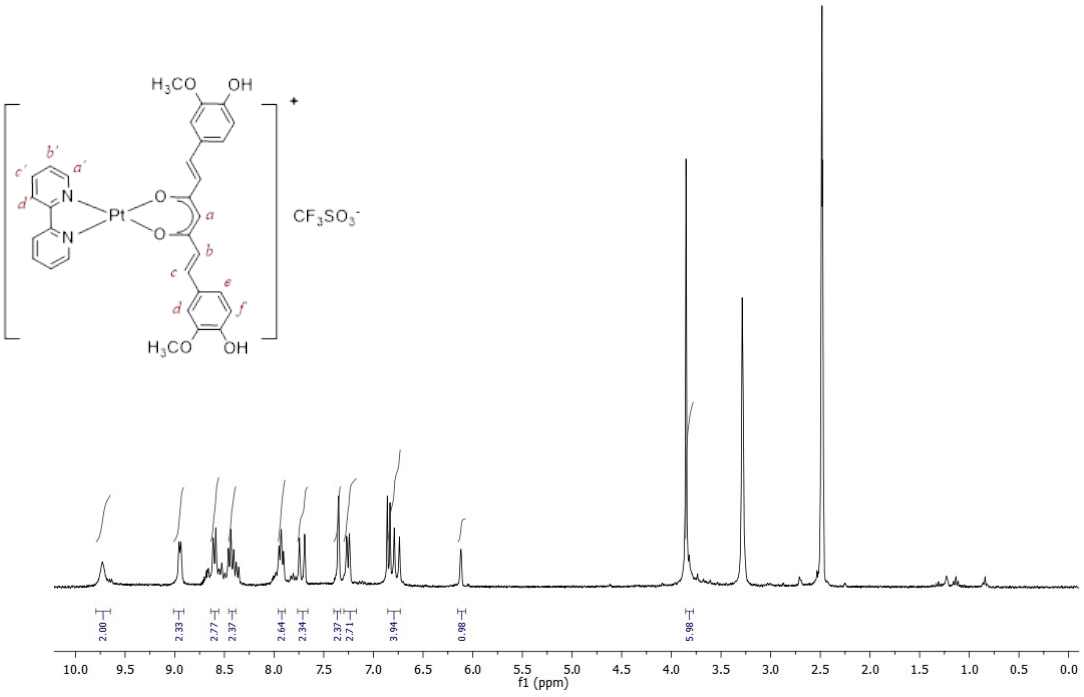

Figure S11: ^{1}H-NMR spectrum of complex [(bipy)Pt(curc)][CF_3SO_3], **3**.

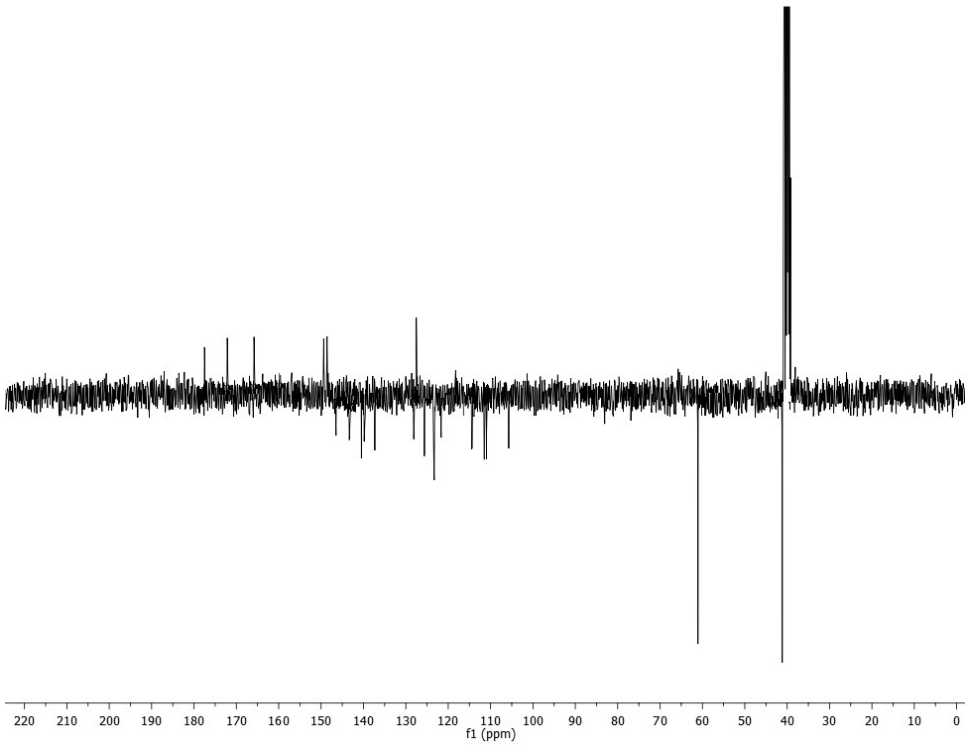

Figure S12: ^{13}C-NMR spectrum of complex [(bipy)Pt(curc)][CF_3SO_3], **3**.

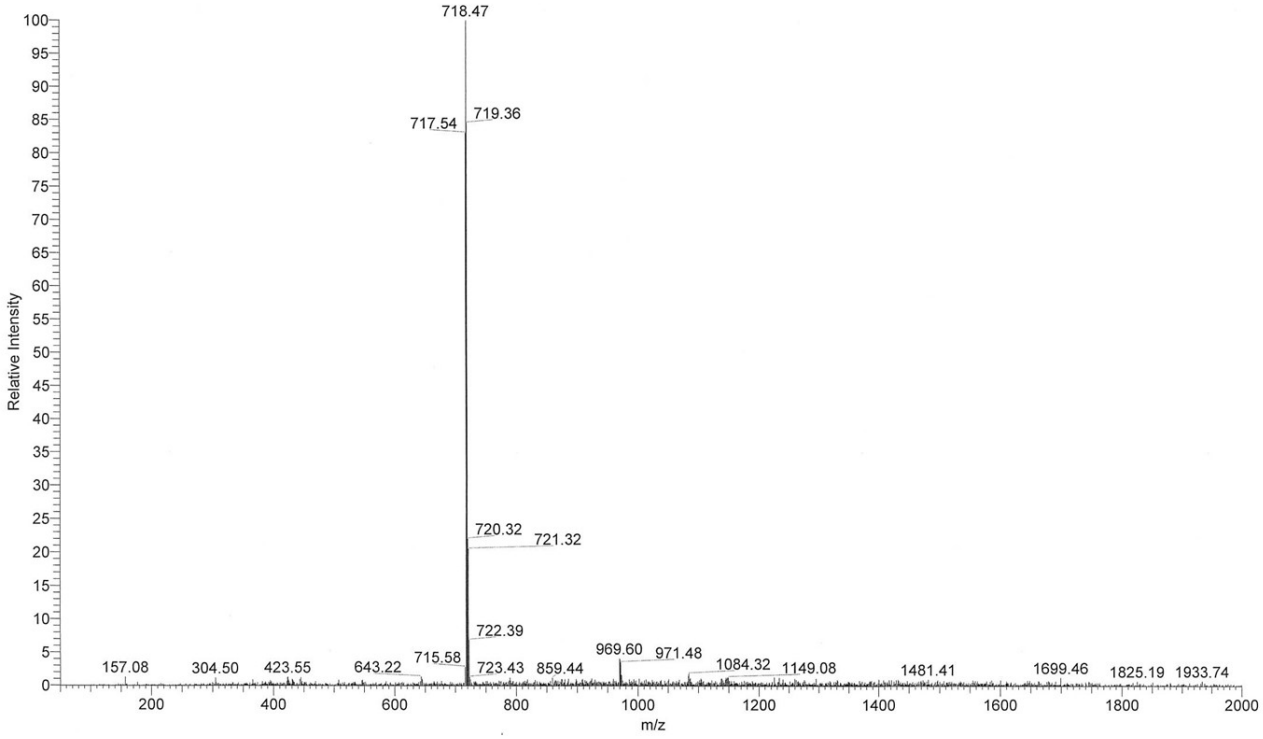

Figure S13: MS spectrum of complex[(bipy)Pt(curc)][CF_3SO_3], **3**.

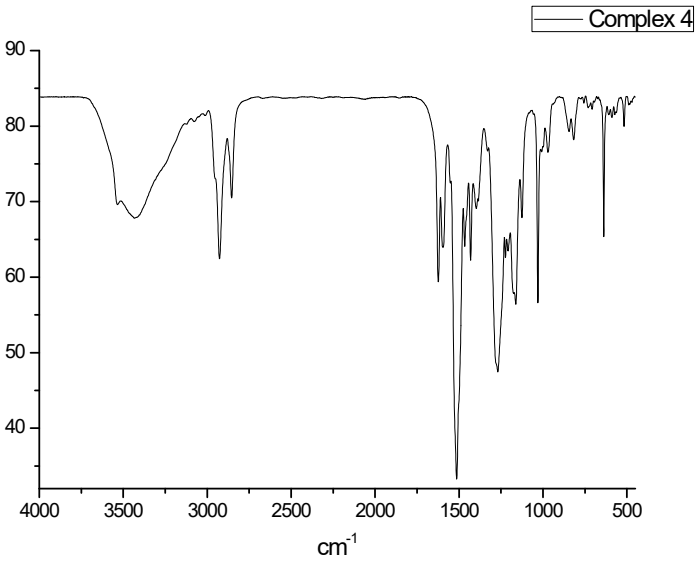

Figure S14: FT-IR spectrum of complex [(bipy-C_9)Pt(curc)][CF_3SO_3], **4**.

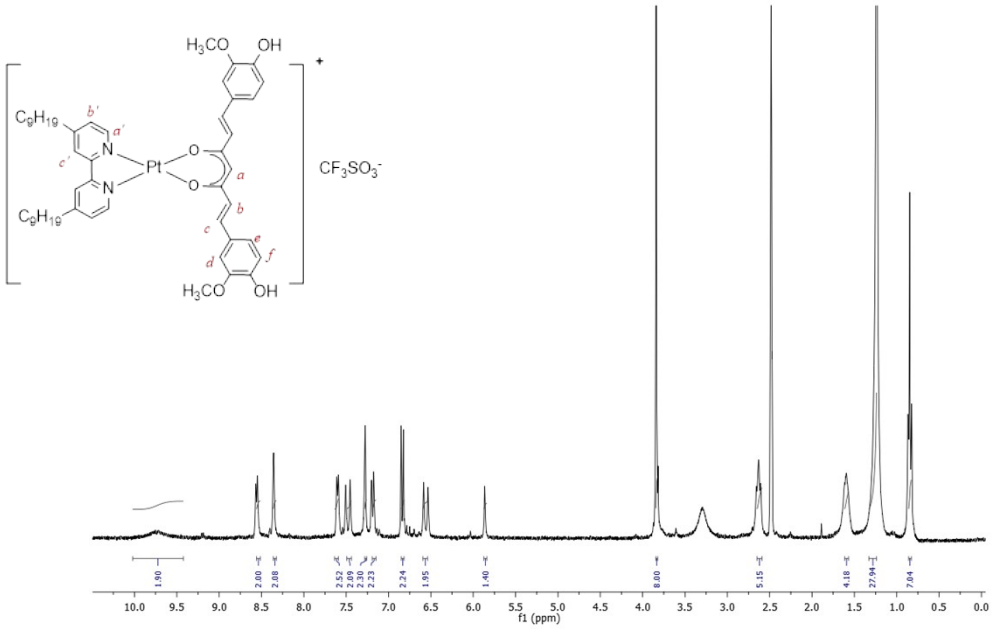

Figure S15: ^{1}H-NMR spectrum of complex [(bipy-C_9)Pt(curc)][CF_3SO_3], **4**.

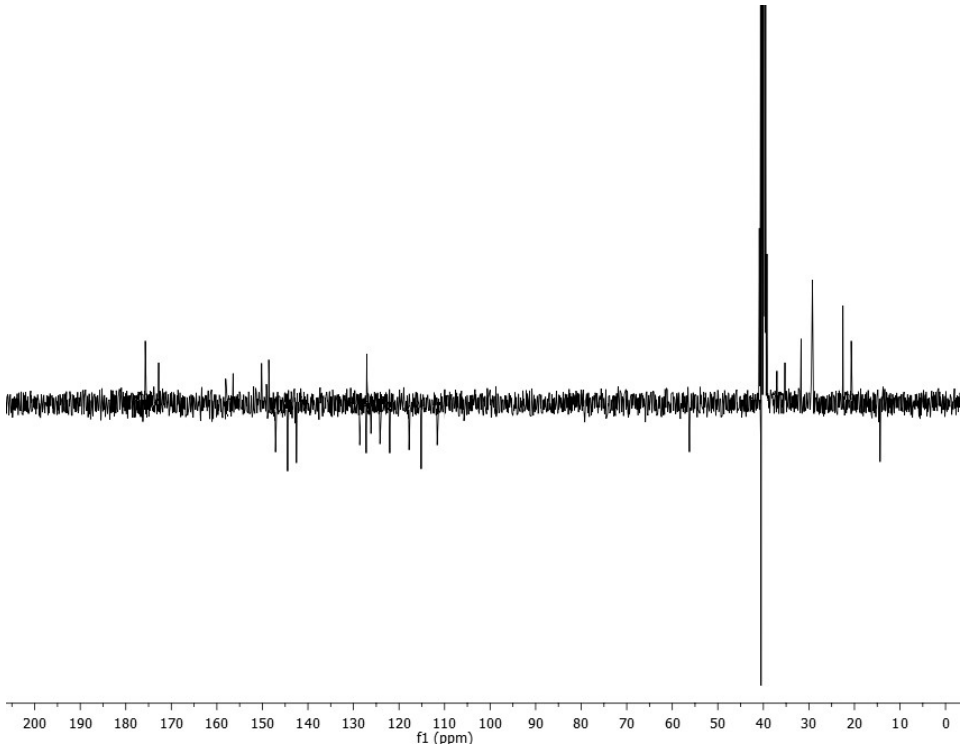

Figure S16: ^{13}C-NMR spectrum of complex [(bipy-C_9)Pt(curc)][CF_3SO_3], **4**.

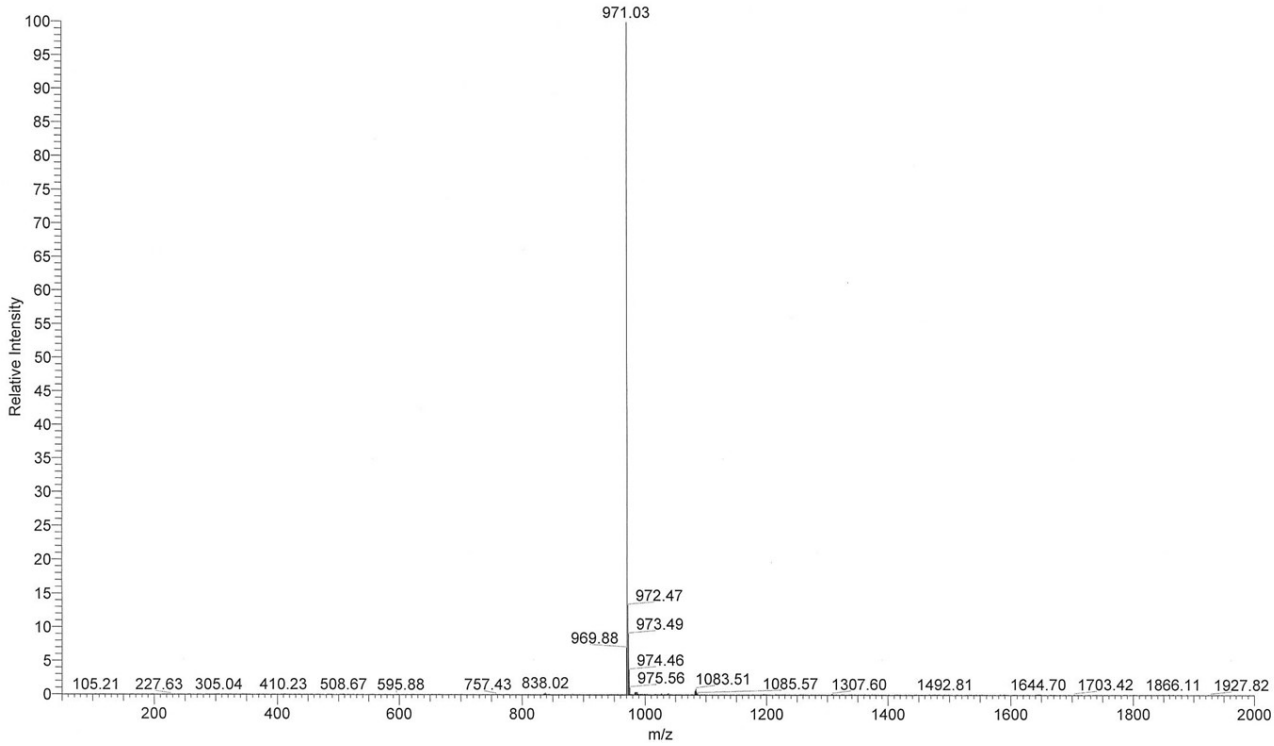

Figure S17: MS spectrum of complex [(bipy-C_9)Pt(curc)][CF_3SO_3], **4**.

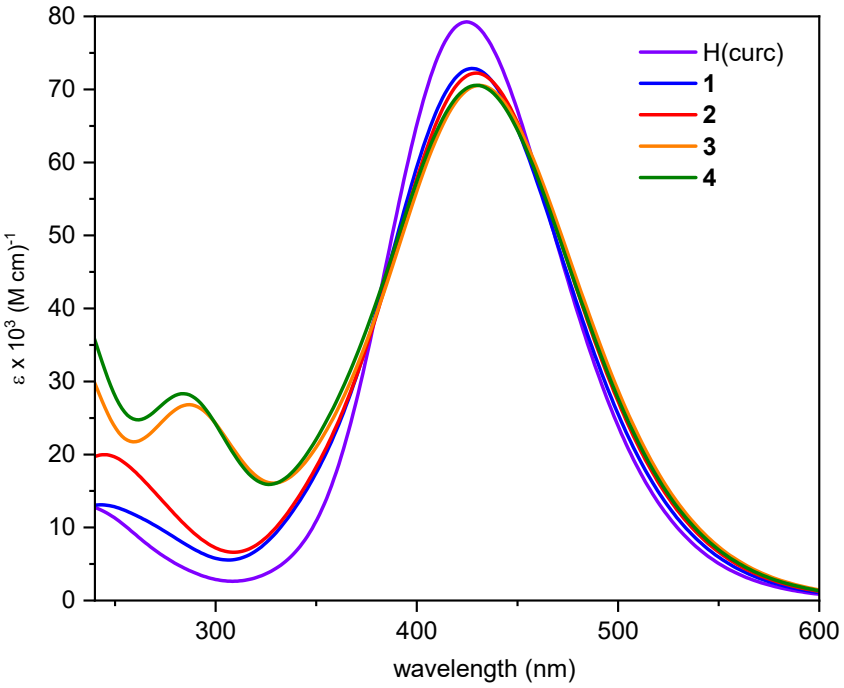

Figure S18: Simulated absorption spectra of **H(curc)** (violet) and complexes **1** (blue), **2** (red), **3** (orange) and **4** (green) in implicit solvent methanol.

Table S1: Absorption wavelength (λ, nm), oscillator strength (f), MO contribution (%) for H(curc) and its Pt(II) cationic complexes **1-4**.

Comp	Band	λ	f^a	MO contribution[b]	Theoretical Assignment
H(curc)	**I**	425	1.949	H → L 94%	ππ*
	II	257	0.105	H-1 → L+1 67%	ππ*
		243	0.107	H → L+3 34%	
				H-1 → L+2 18%	
1	**I**	430	1.749	H → L 93%	LMCT
		361	0.308	H-1 → L 93%	LC/MLCT
	II	259	0.122	H-1 → L+1 57%	MLCT/LC_{curc}
				H → L+3 16%	
2	**I**	432	1.725	H → L 93%	LMCT
		363	0.349	H-1 → L 92%	LC/MLCT
	II	260	0.130	H-1 → L+2 41%	MLCT/LC_{curc}
3	**I**	435	1.665	H → L 93%	LMCT
		366	0.417	H-1 → L 89%	LC/MLCT
	II	307	0.131	H-2 → L+1 40%, H-4 → L+1 33%	LC_{bipy}
		293	0.309	H-5 → L+1 70%	$L_{curc}L_{bipy}CT$
4	**I**	434	1.657	H → L 93%	LMCT
		366	0.441	H-1 → L 90%	LC/MLCT
	II	303	0.180	H-2 → L+1 36%, H-3 → L 25%,	LC_{bipy}
				H-4 → L+1 20%	
		287	0.344	H-5 → L+1 61%	$L_{curc}L_{bipy}CT$

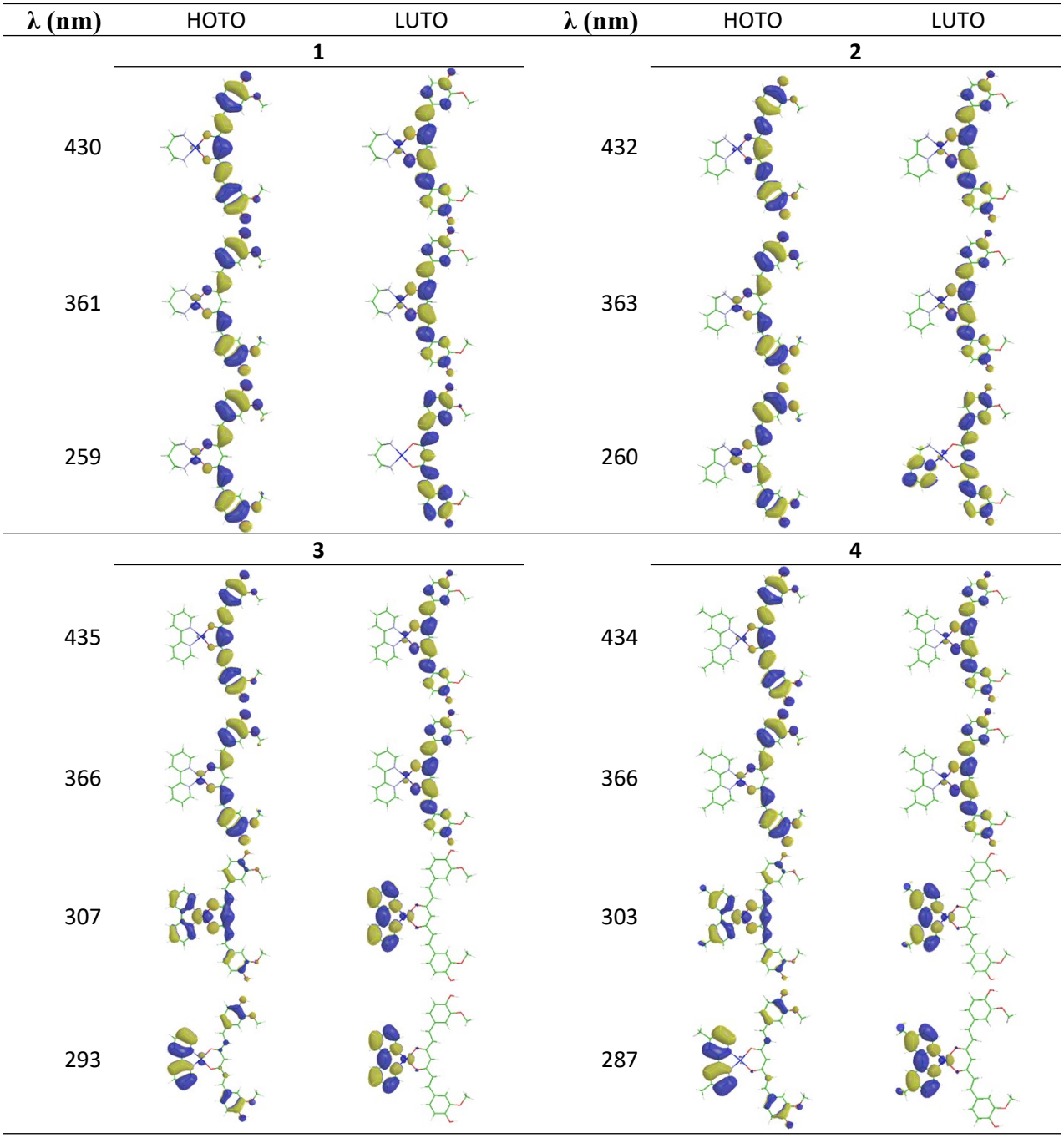

Figure S19: Natural Transition Orbitals (NTOs) for the main excitations of Pt(II) complexes **1**-**4**.

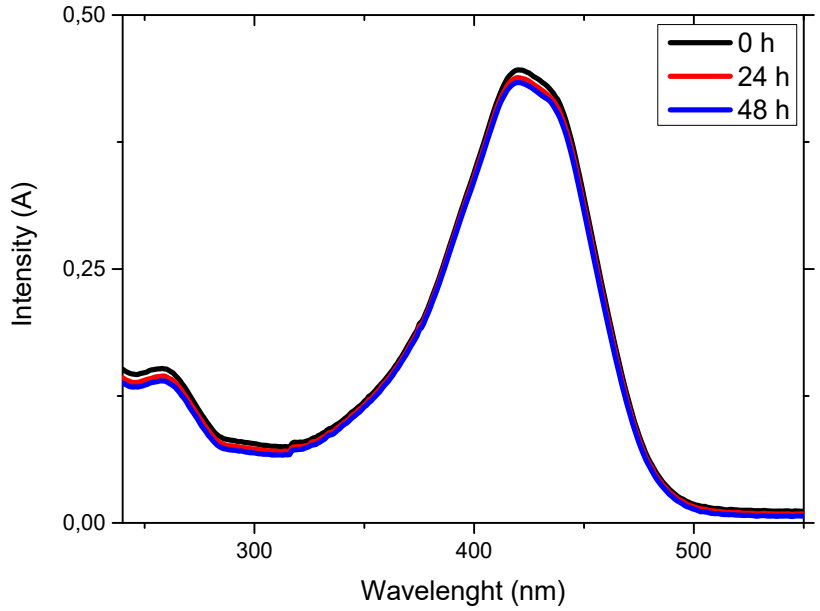

Figure S20: Absorption spectra of **H(curc)** in MeOH dilute solution (10 µM) varying time.

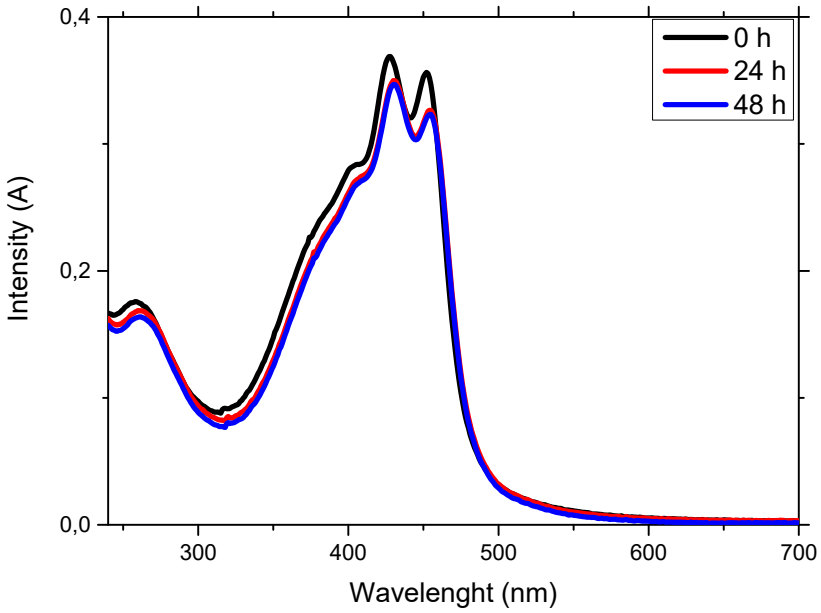

Figure S21: Absorption spectra of complex **1** in MeOH dilute solution (10 µM) varying time.

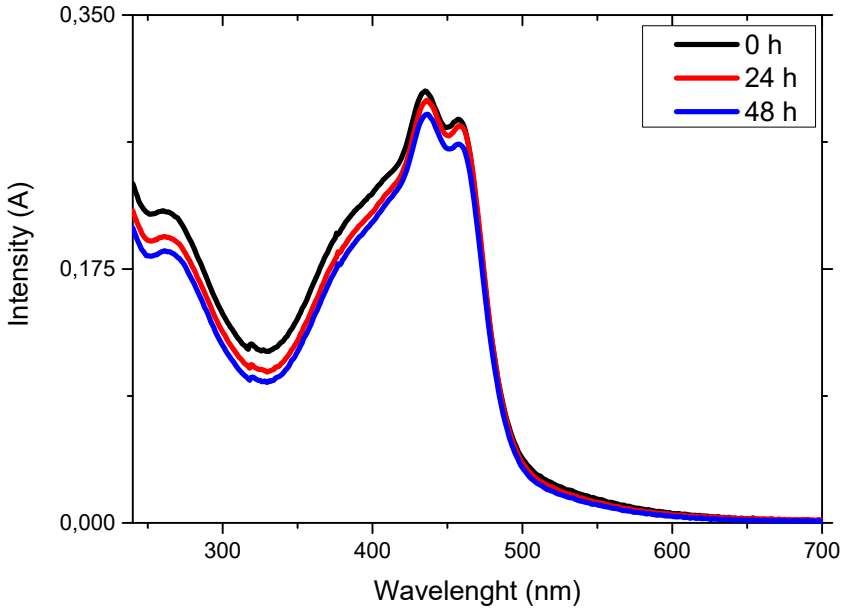

Figure S22: Absorption spectra of complex **2** in MeOH dilute solution (10 µM) varying time.

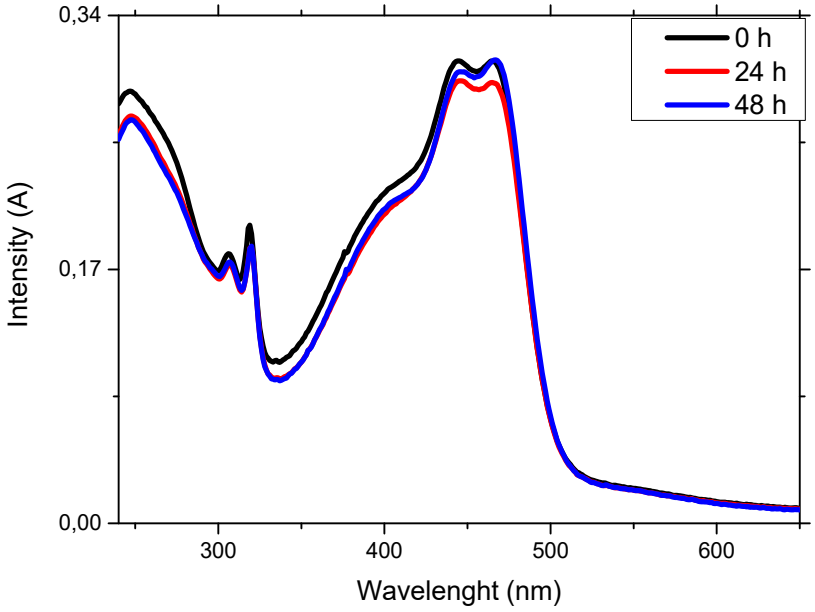

Figure S23: Absorption spectra of complex **3** in MeOH dilute solution (10 µM) varying time.

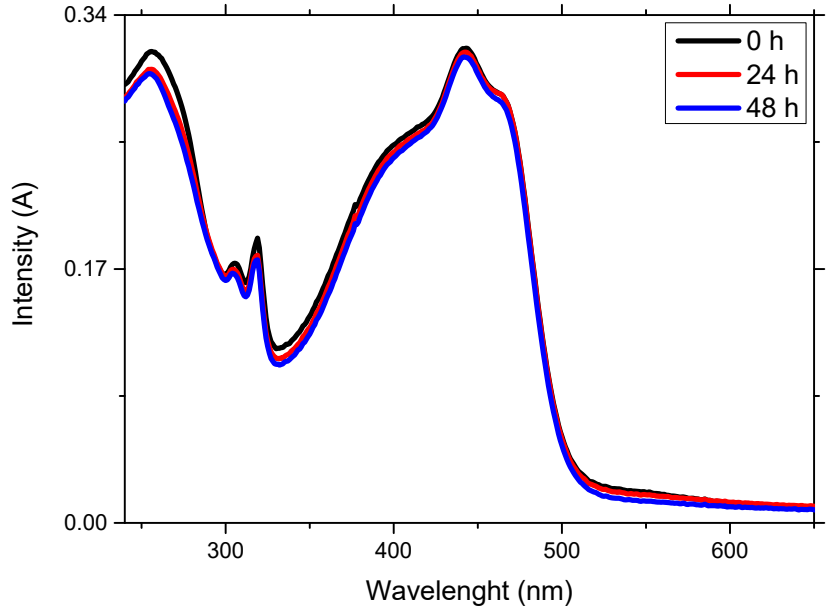

Figure S24: Absorption spectra of complex **4** in MeOH dilute solution (10 µM) varying time.

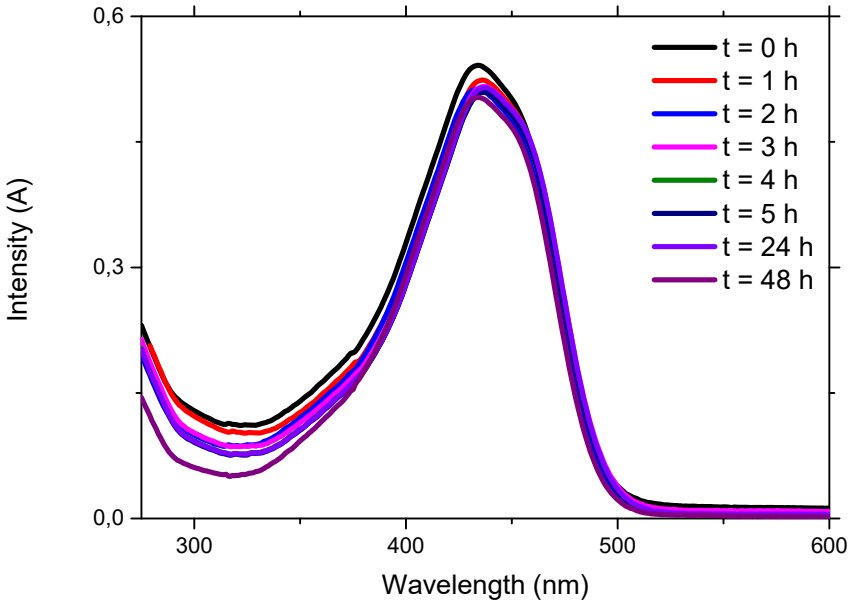

Figure S25: Absorption spectra of **H(curc)** in DMSO dilute solution (10 µM) varying time.

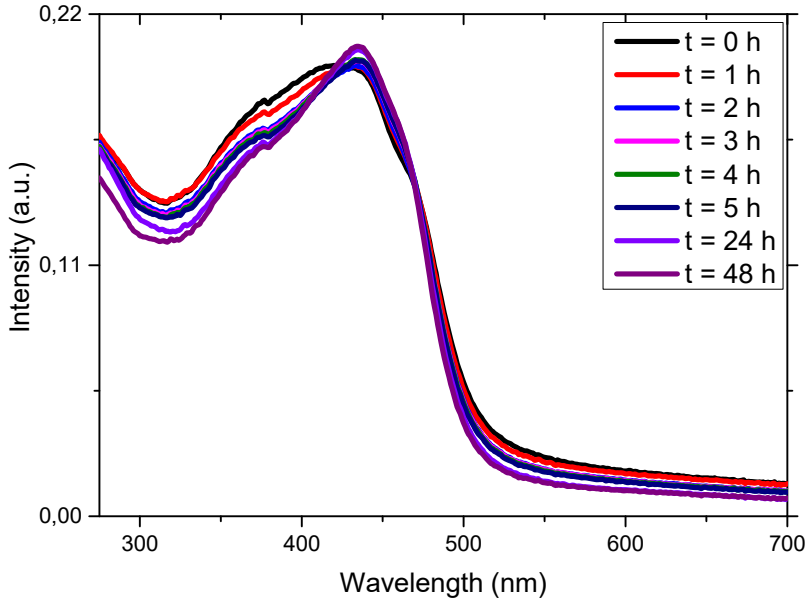

Figure S26: Absorption spectra of complex **1** in DMSO dilute solution (10 µM) varying time.

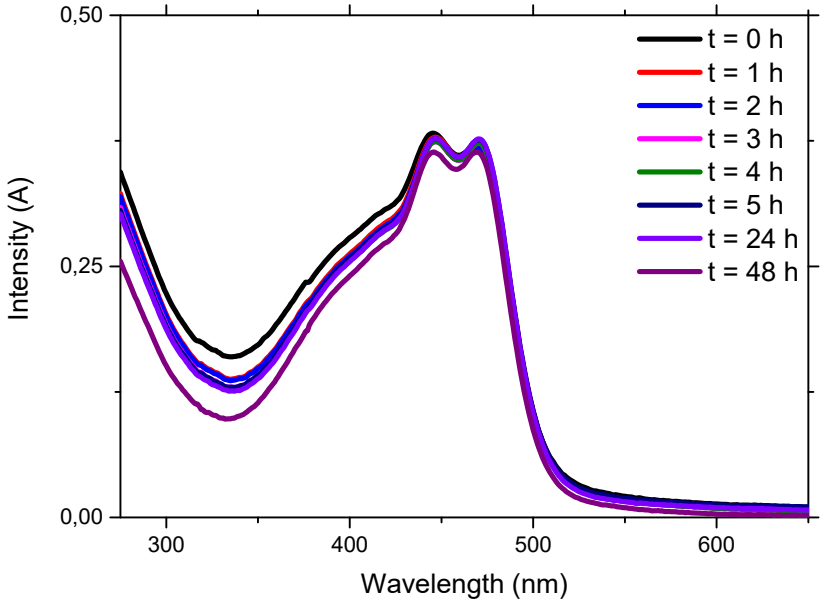

Figure S27: Absorption spectra of complex **2** in DMSO dilute solution (10 µM) varying time.

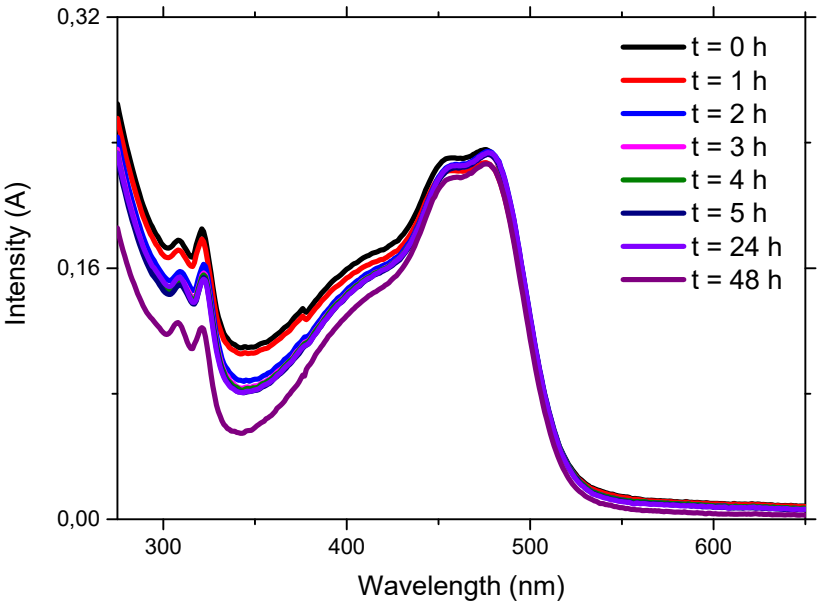

Figure S28: Absorption spectra of complex **3** in DMSO dilute solution (10 µM) varying time.

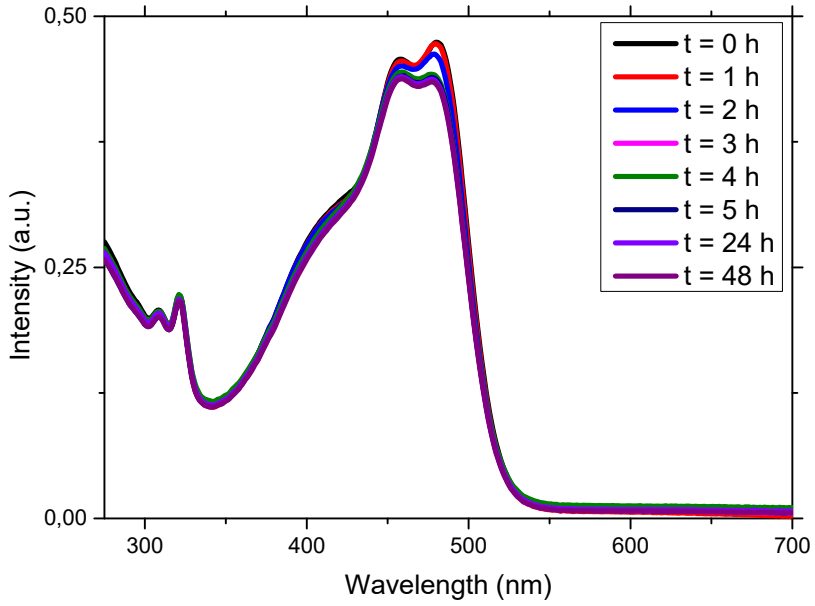

Figure S29: Absorption spectra of complex **4** in DMSO dilute solution (10 µM) varying time.

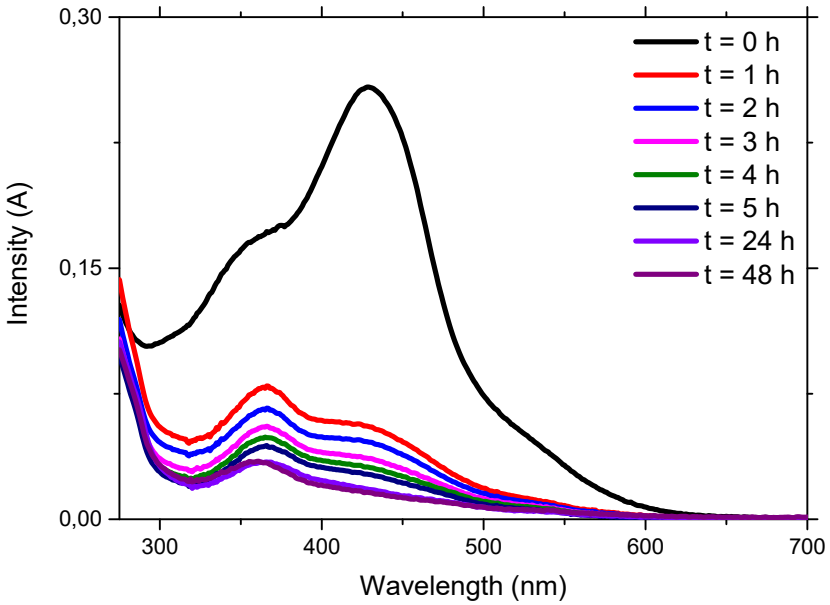

Figure S30: Absorption spectra of **H(curc)** in 10% DMSO/PBS dilute solution (10 µM) varying time.

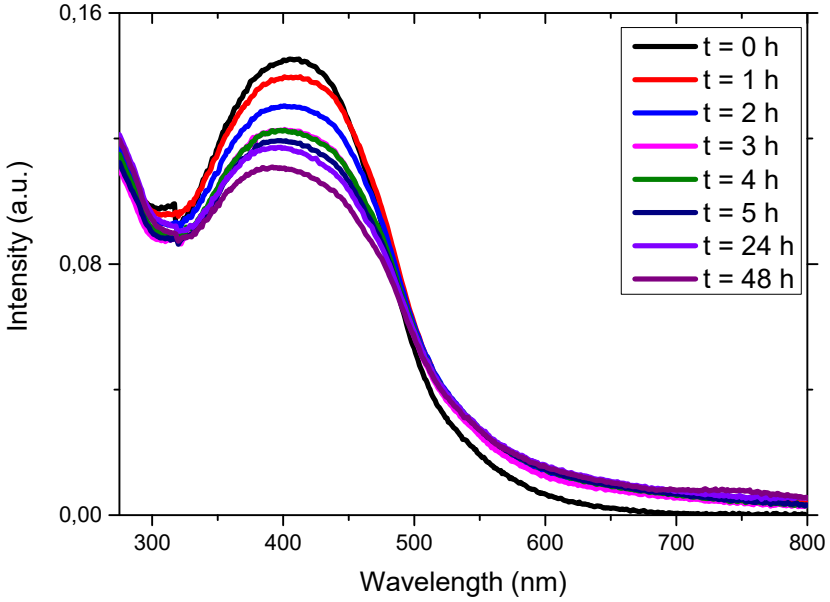

Figure S31: Absorption spectra of complex **1** in 10% DMSO/PBS dilute solution (10 µM) varying time.

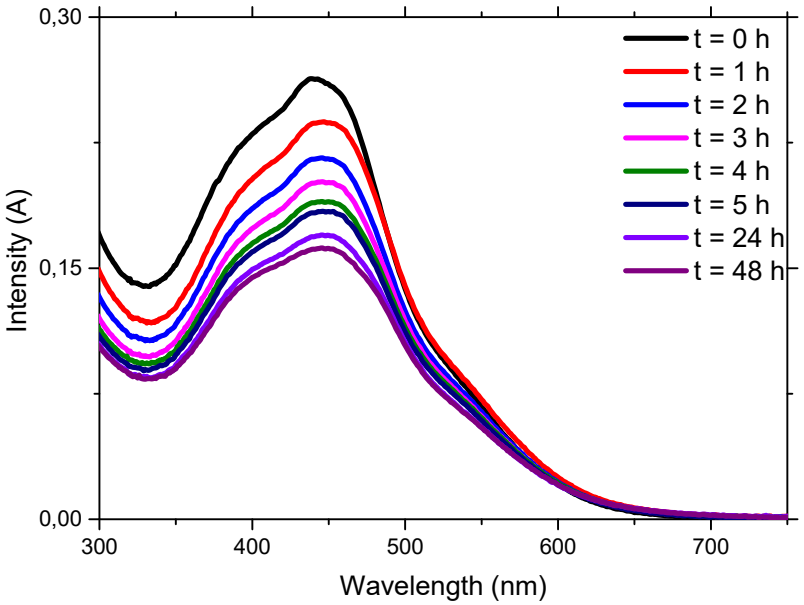

Figure S32: Absorption spectra of complex **2** in 10% DMSO/PBS dilute solution (10 µM) varying time.

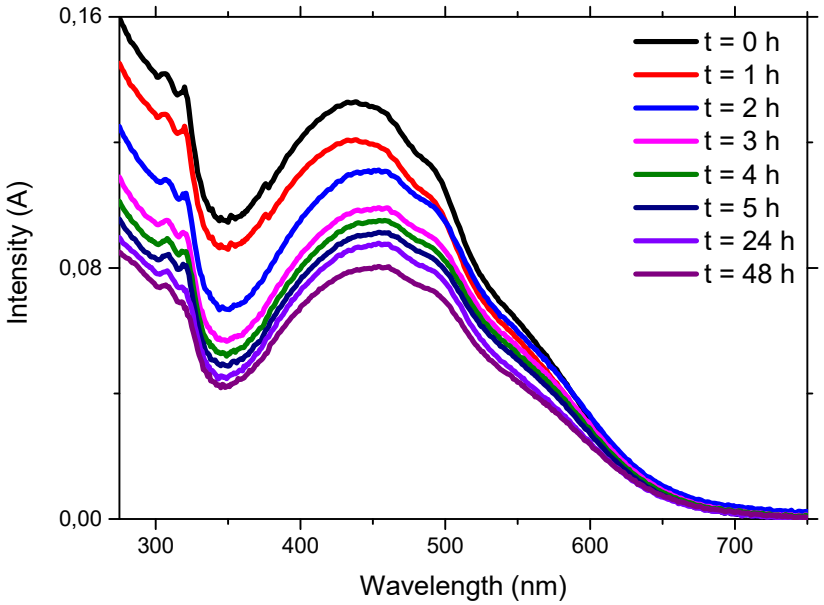

Figure S33: Absorption spectra of complex **3** in 10% DMSO/PBS dilute solution (10 µM) varying time.

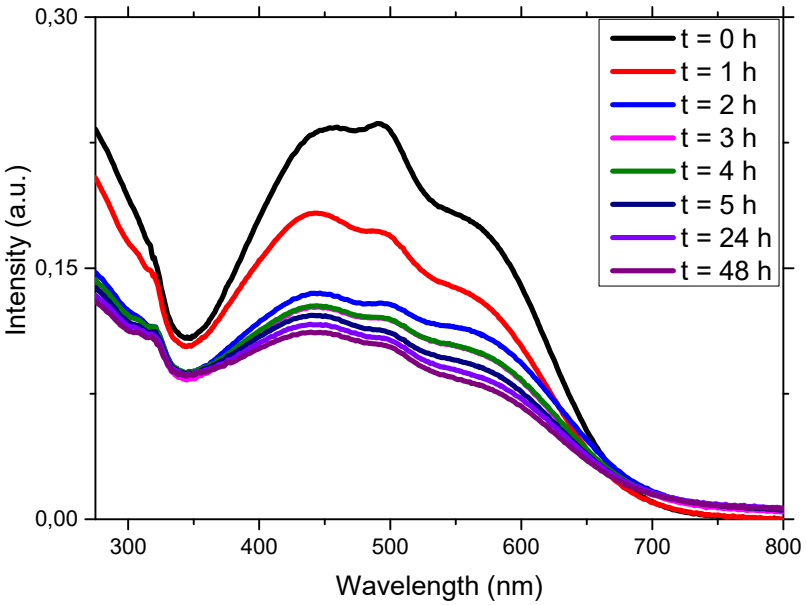

Figure S34: Absorption spectra of complex **4** in 10% DMSO/PBS dilute solution (10 µM) varying time.

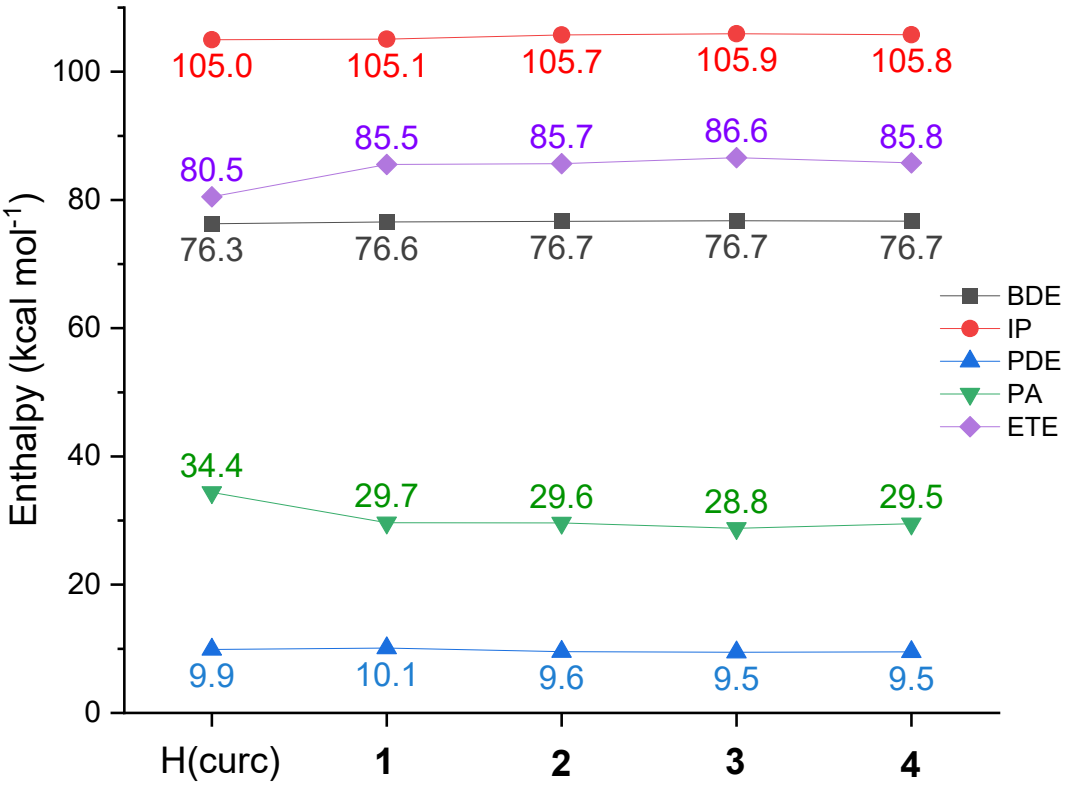

Figure S35: Thermodynamic parameters: bond dissociation enthalpies (BDE, grey), electron transfer enthalpies (ETE, light violet), adiabatic ionization potentials (IP, red), O–H proton dissociation enthalpies (PDE, blue) and proton affinities (PA, green), at 298.15 K.

Table S2: ADME properties of the Pt(II) complexes **1**-**4**.

	1	**2**	**3**	**4**
MW (g/mol)	636.57	670.59	718.63	971.11
H-bond acceptors	6	6	6	6
H-bond donors	4	3	2	2
TPSA (Å)	126.28	113.55	92.98	100.82
LogS	-5.88	-6.67	-7.96	-14.11
GI absorption	High	High	High	Low
BBB permeant	No	No	No	No
Lipinski #violations	1	1	1	2
Bioavailability Score	0.56	0.56	0.56	0.56

Table S3. Theoretical and experimental $logP_{ow}$ values of the Pt(II) complexes **1**-**4**.

	1	**2**	**3**	**4**
$LogP_{ow}^{theo}$	-0.32	0.89	2.69	8.01
$logP_{ow}^{exp}$	2.79	3.22	3.65	8.12

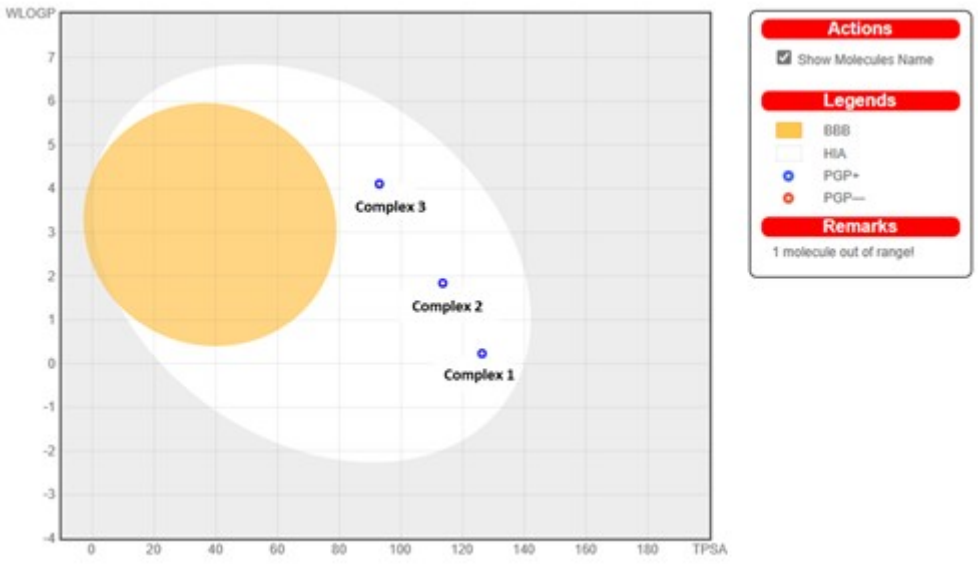

Figure S36: BOILED-Egg Model of complexes **1**-**3**.

	Complex Concentration (μg/μL)					
	0.05	0.1	0.2	0.3	0.4	0.5
H(curc)	0	0.20 ± 0.5	0.60 ± 0.4	0.80 ± 0.1	1.35 ± 0.3	1.99 ± 0.1
1	0.50 ± 0.3	0.90 ± 0.1	1.25 ± 0.1	1.78 ± 0.1	2.11 ± 0.2	2.31 ± 0.2
2	0.50 ± 0.2	1.08 ± 0.1	1.40 ± 0.2	2.10 ± 0.1	2.40 ± 0.1	2.60 ± 0.1
3	0.97 ± 0.3	1.50 ± 0.2	1.70 ± 0.3	2.45 ± 0.2	2.70 ± 0.2	2.88 ± 0.1
4	1.57 ± 0.5	2.00 ± 0.3	2.55 ± 0.2	2.67 ± 0.1	2.93 ± 0.2	3.12 ± 0.1
DMSO	0	0	0	0	0	0

	Complex Concentration (μg/μL)					
	0.05	0.1	0.2	0.3	0.4	0.5
H(curc)	0	0	0	0.80 ± 0.2	1.30 ± 0.1	1.80 ± 0.2
1	0	0.26 ± 0.1	0.52 ± 0.4	1.08 ± 0.2	1.6 ± 0.4	2.06 ± 0.1
2	0	0	0.30 ± 0.2	0.60 ± 0.3	0.80 ± 0.2	1.00 ± 0.4
3	0	0.15 ± 0.2	0.80 ± 0.5	1.40 ± 0.04	1.90 ± 0.3	2.37 ± 0.1
4	0	0.40 ± 0.1	0.60 ± 0.3	1.80 ± 0.6	2.50 ± 0.2	3.00 ± 0.1
DMSO	0	0	0	0	0	0

Table S4: Antimicrobial activity data against *E. coli* (on the top) and *S. aureus* (on the bottom). The diameter(mm) of growth inhibition area is subtracted from the disk diameter (6mm). The values are the mean of three replicates ± standard deviation. 0= no alone.

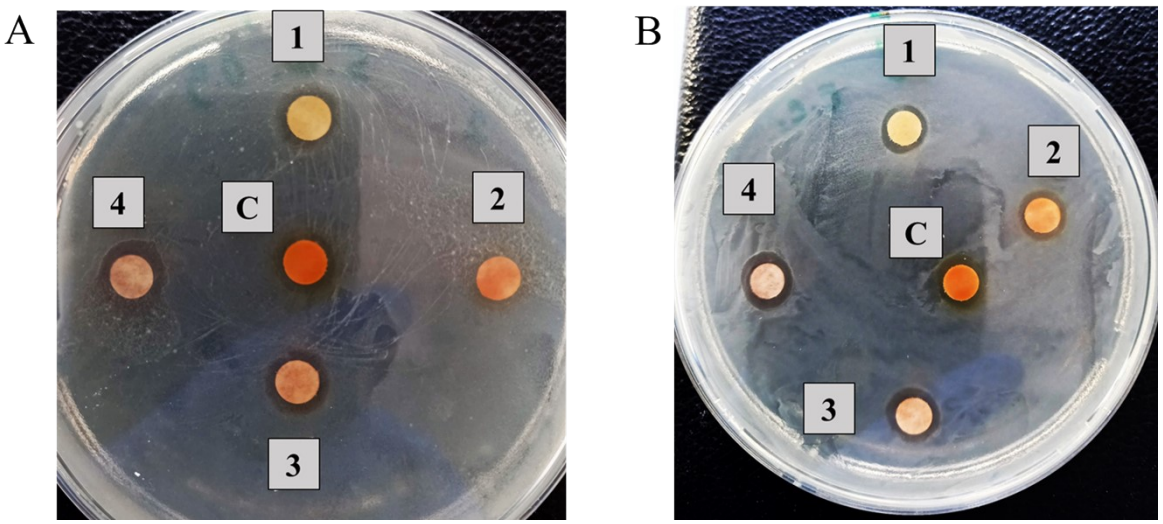

Figure S37: Inhibition halos on *S. aureus* (A) and *E. Coli* (B) at 0.5 µg/µl. C: H(curc).